Enhancing the Radiation Resistance of Undulator Permanent Magnets by Tilting the Easy Axis of Magnetization

Teruhiko Bizen,[1] Ryota Kinjo,[2] and Takashi Tanaka[2,*]

[1]*Japan Synchrotron Radiation Research Institute, Koto 1-1-1, Sayo, Hyogo 679-5198, Japan*

[2]*RIKEN SPring-8 Center, Koto 1-1-1, Sayo, Hyogo 679-5148, Japan*

(Received 7 June 2018; published 17 September 2018)

The undulator is a magnetic device usually consisting of a series of rare-earth permanent magnets (REPMs) arranged to generate a sinusoidal magnetic field, and is installed in synchrotron radiation and free electron laser facilities to periodically deflect high-energy electrons. Because the undulator is operated under a high-radiation environment, it is important to take possible measures to avoid the quality degradation, in particular the radiation damage of REPMs. We present a simple scheme to enhance the radiation resistance of REPMs in undulators, in which the easy axis of each REPM is tilted by 45°. Experimental studies have revealed that the radiation resistance of REPMs in this configuration is enhanced by an order of magnitude compared to that in the conventional undulator.

DOI: 10.1103/PhysRevLett.121.124801

Permanent magnets (PMs), in particular rare-earth PMs (REPMs), have two important advantages over electromagnets: REPMs do not consume any electricity and can generate a much stronger magnetic field than electromagnets having the same volume, as long as the target area is not too wide. Because of these advantages, REPMs have been used in various fields instead of electromagnets. Among them, one of the most important applications is to produce intense synchrotron radiation (SR) as a light source; high-energy electrons are deflected many times by a series of small REPMs arranged to generate a sinusoidal magnetic field, which is usually referred to as an undulator. Nowadays, so many undulators are in operation in SR and free electron laser (FEL) facilities worldwide to produce bright light in wavelength regions that cannot be covered by conventional optical lasers.

It is well known that there are two major REPM materials: samarium-cobalt (SmCo) and neodymium-iron-boron (NdFeB). Although both REPM materials are potentially available for undulators, NdFeB has three major advantages over SmCo: higher (nearly 20%) remanent field, lower cost, and much better mechanical property (less brittle), the last of which is particularly important because we need to handle a huge number of REPM blocks during assembly. As a result, NdFeB is much more attractive than SmCo for undulators, and thus has been used as the primary REPM material and will keep on playing an important role.

One concern in using NdFeB REPMs for undulators is the high radiation dose coming from the high-energy electrons. In contrast to SmCo REPMs, which are highly resistant against radiation, NdFeB REPMs can be easily damaged, or they can be more or less "demagnetized" by radiation. We need to refurbish or replace the undulator if the performance degradation due to demagnetization of REPMs is too serious. Thus, the rate of progress in radiation-induced demagnetization (demagnetization rate) is directly linked to the lifetime of the undulator, which is the reason why many experimental studies have been made to quantify the demagnetization rate of REPMs [1–9].

Recently, we have reported that the demagnetization rate of REPMs in short-period undulators operated in the SPring-8 Angstrom Compact Free Electron Laser (SACLA) [10], one of the running x-ray FEL facilities, is much higher than that of a single REPM placed alone in the radiation environment [11]. Through theoretical and experimental studies, we have revealed that the radiation-induced demagnetization is a highly nonlinear process with respect to the reverse field applied on individual REPMs; in other words, the demagnetization process is accelerated by the strong reverse field, which is intrinsic to the magnetic circuit of conventional undulators.

The above problem is more serious for shorter-period undulators, in which REPMs should be put closer to the electron beam to apply a stronger magnetic field, and thus the number of electrons to hit the REPMs tends to be larger. This suggests that shortening the undulator period, which brings many advantages such as the higher brightness and wider wavelength tunability, potentially leads to a significant reduction in the undulator lifetime. The purpose of this Letter is to present a simple scheme to enhance the radiation resistance of NdFeB REPMs and extend the undulator lifetime.

Let us first explain the magnetic structures of undulators. Figures 1(a) and 1(b) show cross sections of two conventional undulator magnetic arrays: the empty rectangles mean REPM blocks, while the solid ones in Fig. 1(a) mean pole pieces made from a material having high

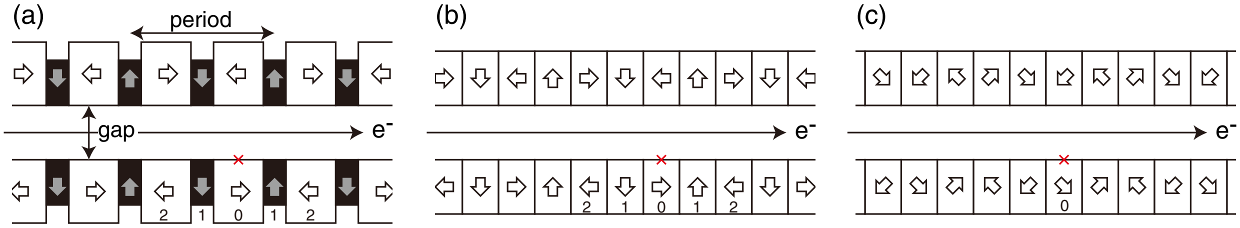

FIG. 1. Cross sections of magnetic arrays: (a) hybrid, (b) normal Halbach, (c) 45° Halbach undulators.

saturated magnetic flux. Empty arrows indicate the directions of magnetization of REPM blocks, while the solid (gray) ones indicate those of the pole pieces. The undulators consisting of these magnetic arrays are usually referred to as the (a) hybrid and (b) Halbach undulators. The latter has been named after its inventor [12,13], and either of the two arrays is selected according to the boundary conditions and required specifications. The peak magnetic field depends on the gap (g) and period (λ_u) as well as the properties of the REPM and pole piece, and is given by a decaying exponential function of g/λ_u. This means that a shorter-period undulator requires a narrower-gap operation to generate a sufficiently strong peak field, which eventually increases the number of electrons to hit the REPMs.

We now emphasize that all the REPM blocks in the hybrid array (a) are exposed to a strong reverse field. For example, the block numbered “0” is exposed to a reverse field generated by the two blocks numbered “2” besides the self-demagnetizing field. What is more critical is that the reverse field applied on the surface facing the electron beam (inner surface), as indicated by a cross mark (×), is enhanced by the two pole pieces numbered “1”. As reported before [11], this strong reverse field works to accelerate the radiation-induced demagnetization, and the magnetic field generated on the electron beam axis is rapidly lost as the radiation dose increases.

The above problem applies also in the Halbach array (b); the inner surface of the block 0 is exposed to a strong reverse field generated by blocks 1 and 2. Note, however, that the vertically magnetized REPM blocks 1 are exposed to a forward field but not the reverse field. As a result, these REPM blocks are quite resistive against radiation. In total, the demagnetization rate of the Halbach array is expected to be roughly twice lower than that of the hybrid array, which may still not be acceptable in most cases.

To overcome the above difficulty caused by the strong reverse field, we propose a magnetic array as illustrated in Fig. 1(c), which is given by slightly modifying the Halbach array (b), i.e., by tilting the easy axis of magnetization in each REPM block by 45°. It is easy to understand that the reverse field applied on the inner surface of each REPM block is much weaker than the other two arrays (a) and (b). For example, the reverse field applied on the point indicated by the cross mark in Fig. 1(c) amounts to zero, besides the self-demagnetizing field. Although the reverse field increases at positions away from this point, its maximum value is still much lower than those of the two conventional arrays. To distinguish (b) and (c) in the following discussions, the former is referred to as the normal Halbach array, while the latter as the 45° Halbach array. It should be noted that Halbach undulators with the tilted easy axis have been constructed [14] and analyzed [15] before; however, the purpose of these works is completely different from what is discussed here. We also note that the performances of the normal and 45° Halbach arrays are similar; in practice, former analytical studies [15] have revealed that they are identical in terms of the deflection parameter, which is one of the most important parameters to specify the undulator performance.

It should be noted that the contribution from the topside magnets has been neglected in the above discussion. In practice, the reverse field is more or less relaxed by its contribution in each magnetic array, whose effect will be discussed later.

To experimentally demonstrate the above concept, we built three different samples consisting of the hybrid, normal Halbach, and 45° Halbach arrays, to be irradiated with high-energy electron beams to investigate the difference in the demagnetization rate. The structures and dimensions of the samples are illustrated in Figs. 2(a)–2(c), with the empty rectangles indicating the REPM blocks and arrows indicating the directions of magnetization. The REPM is made from NdFeB with the remanent field of 1.2 T and coercivity of 2000 kA/m, which is a common material used in typical short-period undulators. All the magnetic arrays have the identical period of 22 mm and consist of eight REPM blocks. Note that the number of periods of the hybrid array is twice larger than that of the other two arrays because of the fewer number of REPM blocks per period. The 40-mm-long copper block placed in front of the magnetic array is to mimic several components placed at the both ends of the magnetic array; they are required in short-period undulators in which the magnetic arrays are located inside the vacuum chamber to reduce the operational gap as much as possible.

Figure 2(a) shows the top and side views of the sample with the hybrid array, together with the coordinate system; z denotes the longitudinal axis along which the electron beam is injected, while x and y denote the horizontal and

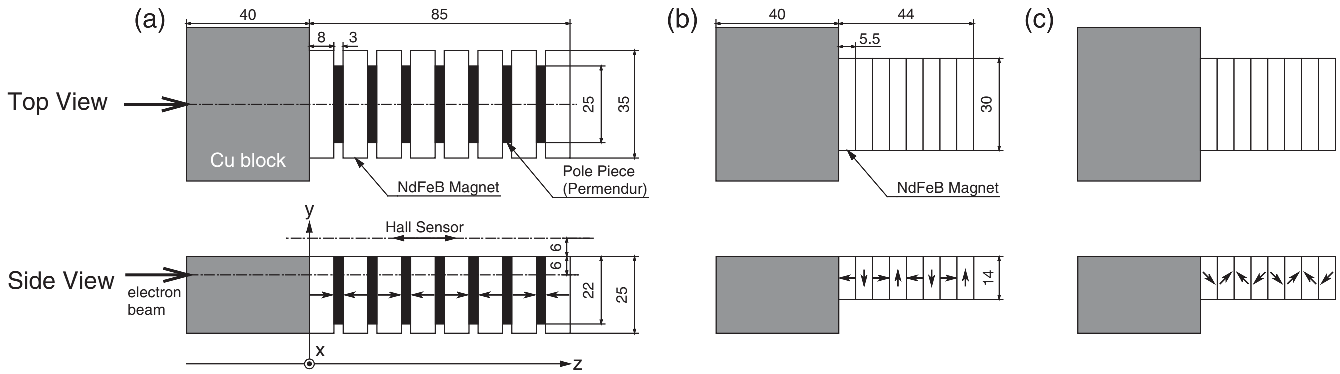

FIG. 2. Structures and dimensions of the undulator samples used for the irradiation experiments, consisting of the (a) hybrid, (b) normal Halbach, and (c) 45° Halbach arrays. The top and bottom figures correspond to the top and side views.

vertical axes perpendicular to z. The solid rectangles indicate the pole pieces made from a cobalt-iron alloy called Permendur, with the saturated magnetic flux of 2.35 T. Figures 2(b) and 2(c) are the same as Fig. 2(a), but for the samples consisting of the normal and 45° Halbach arrays, respectively. Except for the easy axis of magnetization, the two Halbach arrays are identical. In all the samples, the lengths (dimension in z) of the REPM block (and pole piece in the hybrid array) are optimized to maximize the peak magnetic field, while the widths (in x) are chosen to obtain a sufficiently good field uniformity. The heights (in y) are chosen to be long enough so that the resultant peak magnetic field is similar to what is obtained with an infinitely large height. It should be noted that the height of the hybrid array should be nearly twice larger than that of the Halbach arrays. Also note that only the bottom array has been built and irradiated.

Figure 3 shows the magnetic field distributions measured by actuating a Hall sensor along z, 6 mm above the surface of the individual undulator samples as indicated in Fig. 2(a). The origin of z is defined as the edge of the magnetic array for each sample. Although the field distribution is not completely periodic because of the small number of periods, we can clearly define several peaks corresponding to the magnetic poles. Among them, we focus on the second peak indicated by an arrow and evaluate its variation due to irradiation to define the demagnetization.

After measuring the magnetic field distribution, we irradiated each sample with 8-GeV electron beams generated by the synchrotron in the SPring-8 SR facility. The root-mean-square horizontal and vertical sizes of the electron beam, just in front of the sample, were at least smaller than 6 and 1 mm, respectively. The vertical position of irradiation was set 6 mm below the inner surface of the magnetic array as indicated in Fig. 2(a) to make sure that all the electrons in the electron beam, whose current was monitored during irradiation, hit the magnetic array. This allows us to accurately evaluate the demagnetization rate.

Figure 4 shows the results of irradiation, where the demagnetization of each magnetic array is plotted as a function of the number of incident electrons. As expected, the demagnetization rate of the hybrid array is the highest and that of the 45° Halbach array is the lowest, suggesting

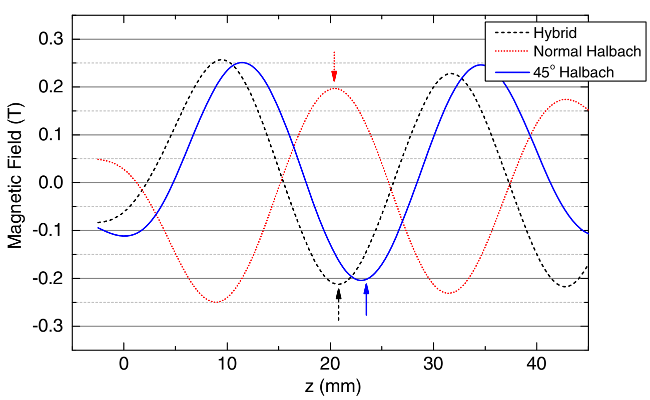

FIG. 3. Magnetic distributions of the three magnetic arrays measured by a Hall sensor along z before irradiation. Arrows indicate the peak positions to evaluate the demagnetization for respective magnetic arrays.

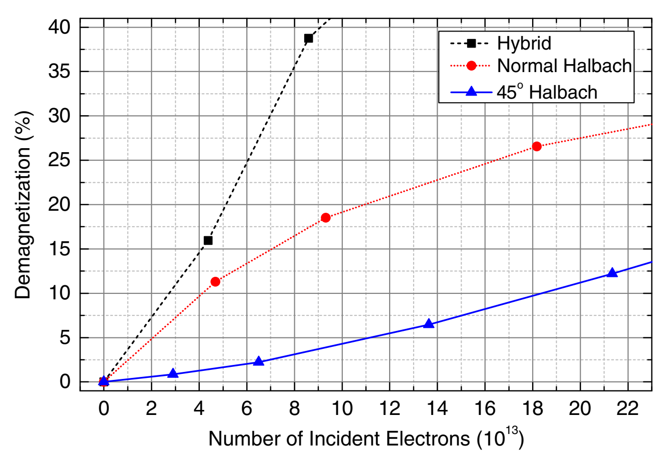

FIG. 4. Demagnetization of each undulator sample evaluated as the variation of the peak magnetic field, plotted as a function of the number of incident electrons.

the strong enhancement of radiation resistance by tilting the easy axis. To be more specific, let us consider the improvement in the undulator lifetime by evaluating the number of electrons N that causes the demagnetization of 5% as an example. Interpolating each curve, we have $N = 1.4 \times 10^{13}$ (hybrid), 2.1×10^{13} (normal Halbach), 1.1×10^{14} (45° Halbach), respectively. This means that the lifetime of the 45° Halbach array is longer than that of the hybrid array by nearly one order of magnitude.

The enhancement of radiation resistance found in the irradiation experiments can be quantitatively explained by the reverse field applied on the REPM blocks. Although it cannot be measured directly, we can numerically evaluate the magnetic field inside the REPM blocks. To facilitate the following discussions, we define the reverse field inside the REPM blocks as $B_{\mathrm{rev}} = -\mu_0 \boldsymbol{H} \cdot \boldsymbol{M}/|\boldsymbol{M}|$, where $\boldsymbol{H}$ is the magnetic field vector, $\boldsymbol{M}$ is the magnetization vector of the REPM, and μ_0 is the vacuum permeability. Note that $\boldsymbol{H}$ should be distinguished from the magnetic flux density $\boldsymbol{B} = \mu_0 \boldsymbol{H} + \boldsymbol{M}$. The reverse field defined above denotes the magnetic field strength projected on the easy axis, and positive values mean that $\boldsymbol{H}$ is oppositely oriented with respect to $\boldsymbol{M}$ and thus works to demagnetize the REPM.

Figures 5(a)–5(c) show the profiles of B_{rev} for the three magnetic arrays calculated along the z axis at two different vertical positions, using the computer code (ANSYS® Electromagnetics Suite, Release 17.1.0, ANSYS, Inc): (i) 6 mm below the inner surface, which was hit by the electron beam in the irradiation experiments, and (ii) exactly on the inner surface. To clarify the calculation conditions, the cross sections of the REPM blocks (and pole pieces) are shown at the bottom, together with the magnetization vectors, in which the vertical positions (i) and (ii) are indicated by the solid and dotted lines, respectively. Note that only the bottom-side magnets are considered in the above conditions (i) and (ii); calculation results under another important condition (ii') are also indicated, which is the same as (ii) except that both-side (top and bottom) magnets are taken into account with the gap of 4 mm. In other words, (ii) is regarded as the special case when the gap is infinitely wide. The origin of z has been redefined as the center of the REPM block, and no data are given for $|z| > 4$ mm in the hybrid array (a), because B_{rev} is defined only inside the REPMs.

To compare B_{rev} between the three magnetic arrays under the conditions in the irradiation experiments, we turn to the profiles (i). We find that B_{rev} of the 45° Halbach array is nearly half of that of the other two arrays within the region of the longitudinally magnetized REPM block, i.e., $|z| < 4$ mm for the hybrid array, and $|z| < 2.75$ mm for the normal Halbach array. This causes a big difference in the demagnetization rate as demonstrated in the irradiation experiments, because of its highly nonlinear dependence on B_{rev}.

In a more realistic condition where the electron beam halo hits the inner surface of the REPM blocks, we need to focus on the profiles (ii) and (ii'). As mentioned before, closing the gap helps to reduce the reverse field, which is evident by comparing the results with (ii) $g = \infty$ and (ii') $g = 4$ mm. In both conditions, B_{rev} of the 45° Halbach array is again much lower than those of the other two arrays, except for the edge of the REPM block. What should be stressed more is the difference in symmetry; B_{rev} is symmetric with respect to the origin of the REPM center ($z = 0$) in the hybrid and normal Halbach arrays, while that of the 45° Halbach array varies as z in an antisymmetric manner. As a result, one of the two edges in the 45° Halbach array located at $z = -2.75$ mm is exposed to a strong forward field ($B_{\mathrm{rev}} < 0$), while both edges are exposed to a strong reverse field in the other two arrays. It is reasonable to expect that this asymmetry helps to enhance the radiation resistance in comparison to the other two conventional arrays.

Finally, we discuss practical effectiveness of the proposed scheme. As a specific example, we consider the demagnetization rate actually observed in one of the

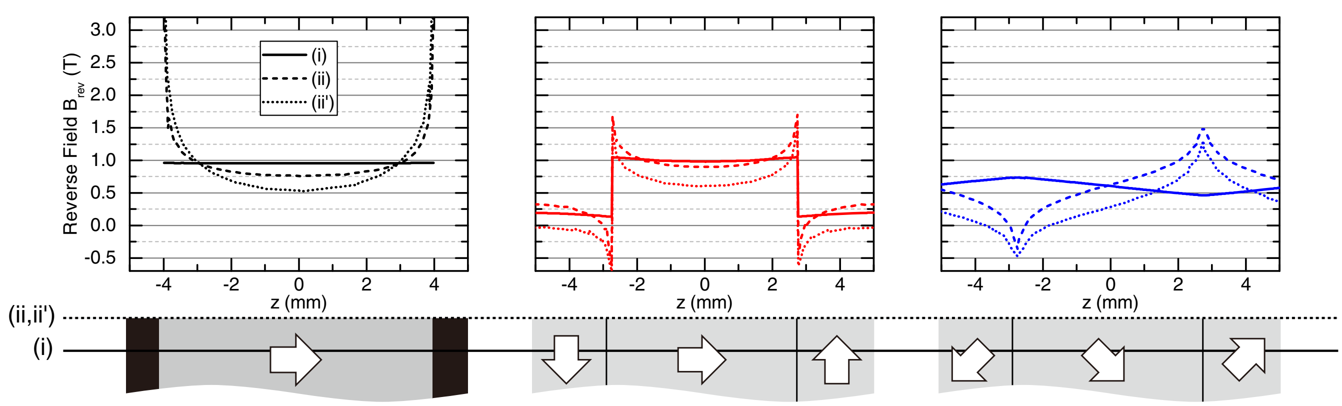

FIG. 5. Profiles of B_{rev} inside the REPM blocks of (a) the hybrid, (b) normal Halbach, and (c) 45° Halbach arrays, calculated along z at the vertical positions (i) 6 mm below the surface, and (ii),(ii') on the surface of each array. The cross sections of REPM blocks are shown at the bottom with the magnetization vectors.

SACLA undulators. As reported in [11], the NdFeB REPMs near the entrance of the most upstream undulator have been demagnetized by at most 35% in the first four years, corresponding to the maximum demagnetization rate of $\sim 10\%/\mathrm{yr}$. Thus, we can expect that the undulator lifetime will be extended by more than 5 yr by applying the proposed scheme, if we define the tolerable demagnetization as being 5%.

It should be noted that the above discussion is not a universal one; the demagnetization rate depends on the boundary condition of each facility such as the electron beam parameters and undulator specifications, and can differ by many orders of magnitude. To keep the demagnetization rate below an acceptable level, we need to take possible actions for (1) reducing the number of electrons incident on REPMs, and (2) enhancing the radiation resistance of REPMs. As a result, we usually have several restrictions on the undulator design, such as the minimum gap and available REPM material, which eventually limit the attainable performance of the undulator. The scheme presented in this Letter offers the third approach to reduce the demagnetization rate, i.e., (3) enhancing the radiation resistance of the magnetic circuit. It goes without saying that this new approach definitely relaxes the specifications required to achieve (1) and (2), and contributes to expanding the operational possibility of FEL and SR facilities.

*ztanaka@spring8.or.jp

[1] T. Bizen, T. Tanaka, Y. Asano, D. Kim, J. Bak, H. Lee, and H. Kitamura, Nucl. Instrum. Methods Phys. Res., Sect. A **467–468**, 185 (2001).

[2] T. Bizen, Y. Asano, T. Hara, X. Marechal, T. Seike, T. Tanaka, H. Lee, D. Kim, C. Chung, and H. Kitamura, Nucl. Instrum. Methods Phys. Res., Sect. A **515**, 850 (2003).

[3] M. Petra, P. D. Hartog, E. Moog, S. Sasaki, N. Sereno, and I. Vasserman, Nucl. Instrum. Methods Phys. Res., Sect. A **507**, 422 (2003).

[4] J. Pflueger, B. Faatz, M. Tischer, and T. Vielitz, Nucl. Instrum. Methods Phys. Res., Sect. A **507**, 186 (2003).

[5] S. Sasaki, M. Petra, I. B. Vasserman, C. L. Doose, and E. R. Moog, in *Proceedings of PAC2005, Knoxville, Tennessee, 2005* (JACoW, Geneva, 2005), pp. 4126–4128.

[6] T. Bizen, Y. Asano, X.-M. Marechal, T. Seike, T. Aoki, K. Fukami, N. Hosoda, H. Yonehara, T. Takagi, T. Hara, T. Tanaka, and H. Kitamura, Nucl. Instrum. Methods Phys. Res., Sect. A **574**, 401 (2007).

[7] J. Skupin, Y. Li, J. Pflueger, B. Faatz, and T. Vielitz, in *Proceedings of EPAC08, Genoa, Italy, 2008* (JACoW, Geneva, 2008), pp. 2308–2310.

[8] P. Vagin, O. Bilani, A. Schops, S. Tripathi, T. Vielitz, and M. Tischer, in *Proceedings of IPAC2014, Dresden, Germany* (JACoW, Geneva, 2014), pp. 2019–2021.

[9] R. Qiu, H.-S. Lee, J. Li, T.-Y. Koo, and T. H. Jang, Nucl. Instrum. Methods Phys. Res., Sect. A **594**, 111 (2008).

[10] T. Ishikawa, H. Aoyagi, T. Asaka, Y. Asano, N. Azumi, T. Bizen, H. Ego, K. Fukami, T. Fukui, Y. Furukawa, S. Goto, H. Hanaki, T. Hara, T. Hasegawa, T. Hatsui, A. Higashiya, T. Hirono, N. Hosoda, M. Ishii, T. Inagaki *et al.*, Nat. Photonics **6**, 540 (2012).

[11] T. Bizen, R. Kinjo, T. Hasegawa, A. Kagamihata, Y. Kida, T. Seike, T. Watanabe, T. Hara, T. Itoga, Y. Asano, and T. Tanaka, Sci. Rep. **6**, 37937 (2016).

[12] K. Halbach, Nucl. Instrum. Methods Phys. Res. **187**, 109 (1981).

[13] K. Halbach, J. Phys. Colloq. C **44**, C1-211 (1983).

[14] T. Tanaka, K. Shirasawa, T. Seike, and H. Kitamura, AIP Conf. Proc. **705**, 227 (2004).

[15] M. Smolyakov, in *Proceedings of the 7th International Conference on Synchrotron Radiation Instrumentation* [*Nucl. Instrum. Methods Phys. Res., Sect. A* 467, 206 (2001)].